

X-ray-Induced Secondary Electron Emission in Porous Materials

P. M. Shikhaliev

*Ioffe Physicotechnical Institute, Russian Academy of Sciences,
Politekhnicheskaya ul. 26, St. Petersburg, 194021 Russia*

Received April 15, 1998

Abstract—Electron emission induced by X-ray radiation in secondary-emission porous materials was investigated. © 2000 MAIK “Nauka/Interperiodica”.

Secondary-emission porous materials are widely used as a working substance in electromagnetic and corpuscular radiation detectors [1–5]. The detection process in this case is governed by the interaction between primary radiation and a porous material, fast-primary-electron and slow-secondary-electron emissions, as well as by avalanche generation and transfer of secondary electrons.

The use of secondary-emission materials in detecting X-ray radiation poses certain difficulties. First, the possibility of the X-quantum–porous medium interaction may be low; and second, X-ray-induced emission is ambiguously related to structure parameters (pore size, pore wall thickness, and pore shape), the chemical composition of the material, and the quantum energy [5–8]. Optimization of the detector performance (in particular, sensitivity improvement) implies the elaboration of a model for X-ray-induced electron emission in porous materials.

In [6–8], electron emission in porous materials was considered for the case of a microchannel plate (MCP) to determine its sensitivity to X-ray radiation. However, the authors used simplified models and failed to discover the effect of the material structure and composition, as well as radiation energy, on the emission.

In this work, we suggest a model of X-rays-induced secondary emission in porous materials with both channel-like and closed pores. The study of closed-pore materials seems to be topical in the context of the development of porous insulator technology [2] and a new type of secondary-emission material—micro-spherical plates [9]. Our model takes into account all structure and composition parameters of the material and possible quantum energies.

The probability P of photon-induced electron emission in a porous body is given by

$$P = P_1 P_2, \quad (1)$$

where P_1 is the probability of quantum–body interaction and P_2 is the probability that a photogenerated or

Compton electron will escape from the wall of a pore into the free space.

The probability P_1 is found from the exponential expression [10]

$$P = 1 - \exp(-\bar{\mu}L), \quad (2)$$

where L is the sample thickness and $\bar{\mu}$ is the mean attenuation coefficient of X-rays in the sample. With regard for porosity,

$$\bar{\mu} = \mu \frac{\bar{\rho}}{\rho}. \quad (3)$$

Here, $\bar{\rho} = \rho(1 - V_0/V)$ is the mean density of the material, ρ is the density of the material, μ is the attenuation coefficient of X-rays in the material, V_0 is the pore volume, and V is the total volume of the sample.

It can be shown [11] that

$$\frac{V_0}{V} = \frac{\alpha}{(1 + w/d)^n}, \quad (4)$$

where $n = 2$ or 3 for channel-like and closed pores, respectively; α is a pore-shape-dependent parameter; and w and d are the mean thickness of the pore wall and the mean pore size.

In view of (3) and (4), we find from (2):

$$P = 1 - \exp\left[-\mu L \left(1 - \frac{\alpha}{(1 + w/d)^n}\right)\right]. \quad (5)$$

The probability P_2 that a fast electron will escape from the wall of a pore into the free space depends on the mean distance from the point of electron generation to the pore surface, electron energy, and chemical composition of the body. Let the mean path of electrons in the wall be x_0 . To find the escape probability, consider a layer of thickness x_0 where N_0 uniformly generated monoenergetic primary electrons move isotropically.

One can show that the number of electrons leaving this layer is [11]

$$N = N_0 \int_0^{x_0} \frac{x}{x_0} dx \int_x^R (1/r^2 + 1/rR) dr. \quad (6)$$

Here, R is the extrapolated range of electrons in the material (it can be found from Tabata's semiempirical equation [12]) and the probability that electrons will pass through an r -thick layer is linearly approximated as $1 - r/R$ [10]. From (6), we obtain the probability P_{21} that a primary electron will leave the wall:

$$P_{21}(x_0) = \frac{N(x_0)}{N_0} = \begin{cases} 1 - \frac{3x_0}{4R} + \frac{x_0}{2R} \ln \frac{x_0}{R} & \text{at } R > x_0 \\ \frac{R}{4x_0} & \text{at } R < x_0. \end{cases}$$

If all primary electrons move normally to the surface,

$$P_{22}(x_0) = \begin{cases} 1 - \frac{x_0}{2R} & \text{at } R > x_0 \\ \frac{R}{2x_0} & \text{at } R < x_0. \end{cases}$$

Primary photogenerated and Compton electrons have known emission-angle distributions, and the true probability $P_2(x_0)$ of their emission lies between $P_{21}(x_0)$ and $P_{22}(x_0)$. It follows from this condition that the dependence $P_2(x_0)$ can be approximated by the exponential function

$$P_2(x_0) = \exp(-kx_0)$$

more convenient for analysis. Here, k has the meaning of absorption coefficient of electrons and obeys the condition $\ln 2 < kR < \ln 4$.

The value of k can be found from the well-known empirical expression [10]

$$k = 17E^{-1.42}, \quad (7)$$

which was derived for the absorption coefficient of unidirectional β -electrons with a continuous energy spectrum and a mean energy equal to the mean energy of primary electrons.

The mean path of electrons in the wall depends on the pore size, pore shape, and pore wall thickness. It can be given by [11]

$$x_0 = \beta d [(1 + w/d)^n - \gamma], \quad (8)$$

where β and γ are parameters dependent on pore shape and arrangement.

Thus, the probability P_2 that primary electrons will escape from the wall into the free space is

$$P_2 = \exp[-\beta kd((1 + w/d)^n - \gamma)]. \quad (9)$$

Note that μ and k in (5) and (9) depend on the X-quantum energy and the composition of the porous body according to known laws. Hence, the derived expression for the probability P_1P_2 of radiation-induced emission of fast electrons in a porous body takes into account all structure and composition parameters of the material and the X-quantum energy. From (5) and (9), it is easy to see that P_1P_2 plotted against w and d exhibit maxima. The dependence of P_1P_2 on quantum energy also peaks if the empirical expression for μ

$$\mu(E) = C \exp(-3.5E) \quad [10]$$

is included in (5).

When fast primary electrons traverse the pores, transmission and reflection secondary electron emissions arise. The number of generated slow secondary electrons is related to the secondary emission coefficient of the material [13] and the number of pores traversed by a primary electron. The latter is expressed as $N = R/x_0$, where R and x_0 are, as previously, the extrapolated range and the mean path of primary electrons in the wall.

Among currently available porous materials, MCPs, including those with channel-like pores, are of most interest for applications. First, MCP parameters can be optimized to obtain the maximum X-rays-induced electron emission and the maximum sensitivity of MCP detectors. Second, the MCP measured sensitivity can be compared with calculated values. In Figs. 1a and 1b, calculated relative emissions in the MCP are plotted against the structure parameters.

It is known that the efficiency of X-quantum detection by an MCP detector depends on the probability that fast primary electrons will be generated and emitted into MCP channels. Calculated (within the suggested model) and experimental [6] efficiencies of the MCP detector vs. X-quantum energy are depicted in Fig. 2.

The MCP material (lead glass) consists of Si, Pb, and O to the extent of 95%. Their relative content may vary within wide limits. These elements, however, enter into the composition as compounds (SiO_2 and PbO) rather than as individual components. Therefore, the weight fraction of one of them (say, lead) specifies those of the other two. This makes it possible to set a correlation between the photo-induced emission in an MCP and the content of one constituent [14]. Figure 3 shows the fast electron emission vs. lead percentage in the MCP material.

With expressions derived for photon-induced electron emission in porous materials, we estimated the efficiency of MCP detectors studied in our previous

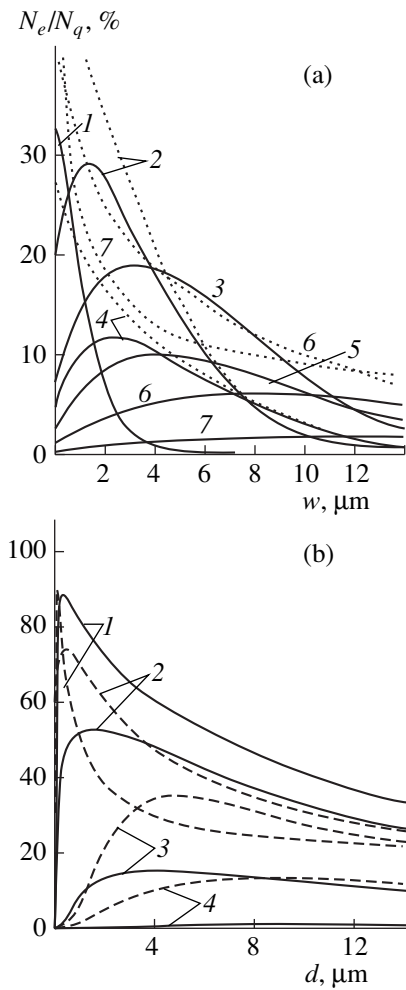


Fig. 1. (a) Relative photon-induced emission of fast (solid lines) and slow (dotted lines) electrons in the MCP vs. channel wall thickness w ; channel diameter $d = 15 \mu\text{m}$: (1) 25, (2) 40, (3) 60, (4) 122, (5) 150, (6) 250, and (7) 662 keV. (b) Relative photon-induced emission in the MCP vs. channel diameter d : $w =$ (1) 0.1, (2) 0.5, (3) 1.5, and (4) 5.0 μm ; solid line, 25 keV; dashed line, 40 keV. $L = 1 \text{ mm}$, MCP thickness; N_e and N_q , the number of electrons and quanta, respectively.

work [3] and elsewhere [7, 8, 15]. Analytic values were compared with experimental data (Fig. 4).

It was found that today's MCP parameters used in detecting X-rays are not optimum. Their optimization with the suggested model may greatly improve MCP sensitivity to X-ray radiation.

It should be noted that our procedure for photon-induced electron emission characterization is also applicable to other porous materials, such as porous insulators and microspherical plates. The latter are a new secondary-emission substance [9], namely, a ~1-mm-thick plate with closely packed glass microspheres of diameter ~40 μm inside. The spheres are covered by a special film with a high secondary emission coefficient. Microspherical plates differ from

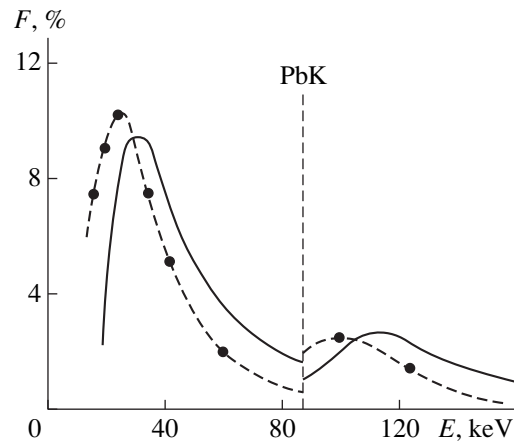


Fig. 2. Analytic (solid line) and experimental (dashed line) dependences of the efficiency of the MCP X-ray detector vs. X-quantum energy.

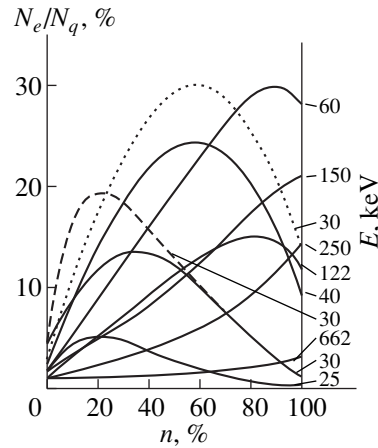


Fig. 3. Relative photon-induced emission of fast electrons against the lead percentage n in the MCP materials; $d = 15 \mu\text{m}$. Solid lines: $L = 1 \text{ mm}$, $w = 3 \mu\text{m}$; dashed line: $L = 3 \text{ mm}$, $w = 3 \mu\text{m}$; dotted line: $L = 1 \text{ mm}$, $w = 1 \mu\text{m}$.

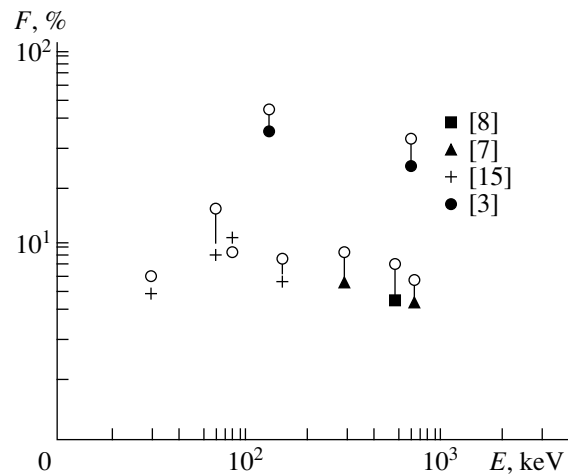


Fig. 4. Calculated (empty circles) and experimental values of the efficiency F of the MCP X-ray detector for different quantum energies E .

MCPs in that avalanche generation of secondary electrons takes place between the spheres.

ACKNOWLEDGMENTS

The author is indebted to B. A. Mamyryn for valuable discussions.

REFERENCES

1. C. Chianelli, P. Aregon, J. Boulet, *et al.*, Nucl. Instrum. Methods Phys. Res., Sect. A **273**, 245 (1988).
2. M. P. Lorikyan, Usp. Fiz. Nauk **165**, 1323 (1995).
3. P. M. Shikhaliev, Rev. Sci. Instrum. **67**, 700 (1996).
4. P. M. Shikhaliev, Nucl. Instrum. Methods Phys. Res., Sect. A **379**, 307 (1996).
5. G. W. Fraser, Nucl. Instrum. Methods Phys. Res., Sect. A **221**, 115 (1984).
6. J. E. Bateman, Nucl. Instrum. Methods Phys. Res., Sect. A **144**, 537 (1977).
7. J. Adams, Adv. Electron. Electron Phys. **22A**, 139 (1966).
8. W. T. A. McKee, A. C. Duffy, W. B. Feller, *et al.*, Nucl. Instrum. Methods Phys. Res., Sect. A **310**, 255 (1991).
9. A. S. Tremsin, J. E. Pearson, J. E. Lees, *et al.*, Nucl. Instrum. Methods Phys. Res., Sect. A **368**, 719 (1996).
10. K. Zigban, *Alpha-, Beta-, and Gamma-Spectroscopy* (Atomizdat, Nauka, 1969).
11. P. M. Shikhaliev, Candidate's Dissertation (St. Petersburg, 1998).
12. T. Tabata, R. Ito, and S. Okabe, Nucl. Instrum. Methods Phys. Res. **103**, 85 (1972).
13. L. G. Dobretsov and M. V. Gamayunova, *Emission Spectroscopy* (Nauka, Moscow, 1966).
14. P. M. Shikhaliev, Rev. Sci. Instrum. **68**, 3676 (1997).
15. R. J. Gould, P. F. Judy, and B. E. Bjarngard, Nucl. Instrum. Methods Phys. Res. **144**, 493 (1977).

Translated by V. A. Isaakyan